Elastomeric Seismic Isolators Behavior at Different Pads Thickness

Gabriele Milani[1] and Federico Milani[2]
[1]*Politecnico di Milano, Piazza Leonardo da Vinci 32, 20133, Milan, Italy*
[2]*Chem. Co Consultant, Via J. F. Kennedy 2, 45030, Occhiobello (RO), Italy*

Keywords: Elastomeric Isolators, Hardness/Young's Modulus, Elastic Modulus/Thickness, Stretch-stress and Shear Behavior under Large Deformations, Numerical Simulations, Finite Element Method.

Abstract: A seismic isolator has the main function to be extremely deformable for horizontal forces, but at same time sufficiently stiff when loaded with vertical actions. These properties may be strongly influenced by both the isolator geometry (i.e. overall dimensions, number and thickness of rubber pads and steel laminas) and the mechanical properties of rubber pads. Mechanical properties of the pads, especially Young modulus, may be evaluated as a function of hardness, by means of consolidated empirical formulas. In this work, the influence of rubber pads thickness and hardness on both vertical and horizontal stiffness of realistic seismic isolators is discussed. Three full 3D Finite Element models referred to three different seismic isolators having different slenderness are analysed in detail in both vertical compression (elastic analysis) and simple shear in large deformations. Uniaxial and shear response of the seismic devices obtained numerically are finally critically compared, with the aim of evaluating the best compound to be used in practice.

1 INTRODUCTION

In the recent past, seismic isolation technology has been applied almost entirely to large buildings in high seismicity countries, where seismic events are expected to be relevant. One of the most diffused technology for seismic isolation is the utilization of elastomeric multilayer bearings. Until now, the high cost of production reduces the use of seismic isolation mainly for important buildings. Their cost is due to the preparation of the steel plates, which are used to provide vertical stiffness, and the assembly of the rubber sheets. From a technical point of view, the rubber has the main function to be extremely deformable for horizontal forces, but at the same time sufficiently stiff when loaded with vertical actions. Each individual elastomeric layer in the bearing deforms according to two kinematic assumptions, i.e. that (1) horizontal planes remain planar and (2) points on vertical lines lie on a parabola after loading.

This is obtained thanks to the incompressibility of the rubber sheets (Amin et al., 2002; 2006, Gracia et al., 2010) and the introduction of the thin reinforcing steel plates, interspersed between 10-30 mm thick rubber pads (Moon et al., 2002; 2003). Kelly and co-workers (e.g. Tsai and Kelly, 2002) have demonstrated that theoretically it is possible to substitute reinforcing elements of multilayer elastomeric isolation bearings, which are normally steel plates, by fiber reinforcement. This solution goes to a drastically reduction in the weight and probably in the reduction of the cost in the assembly of the items. Milani & Milani (2012) have described a numerical approach to predict the macroscopic behavior of parallelepiped elastomeric isolators undergoing large deformations. In that work, the actual behaviour of elastomeric sheets as a function of the typology of rubber used and their compounds were discussed. Following the original approach proposed in Milani & Milani (2012), in the present work, with the aim of reducing the production cost, we have theoretically considered the opportunity to increase the thickness of the rubber sheets and decrease the steel plates. This geometrical rearrangement provides a decrease of the vertical stiffness but at the same time a good performance under horizontal loads. When the rubber pad thickness is increased up to 3.5 cm, it would be necessary to consider the kinetic of vulcanization of the rubbers sheets, in order to obtain mechanical-elastomeric characteristics as homogeneous as possible in any point of the rubber pad. This would allow to obtain responses for horizontal forces of the

Milani G. and Milani F..
Elastomeric Seismic Isolators Behavior at Different Pads Thickness.
DOI: 10.5220/0004012000170023
In *Proceedings of the 2nd International Conference on Simulation and Modeling Methodologies, Technologies and Applications* (SIMULTECH-2012), pages 17-23
ISBN: 978-989-8565-20-4

isolator similar to those obtained with thin sheets. As it is known, the mechanical elastic behavior can be correlated to the density of the cross-link, that is function of the thickness, the dimensions, the type of rubber and the compound. For these reasons, it is necessary to optimize the vulcanization in terms of time/temperature in such a way that in all points of the items there are similar mechanical-elastomeric characteristics and in order to obtain pads with a hardness directly proportional to pad thickness. As a matter of fact, mechanical properties of the pads, especially Young modulus, at a first attempt and without the possibility to perform expensive mechanical simulations, may be evaluated as a function of hardness, by means of consolidated empirical formulas. In this work, the influence of rubber pads thickness and hardness on both vertical and horizontal stiffness of realistic seismic isolators is discussed. Three full 3D Finite Element models referred to three different seismic isolators having different slenderness (and hence thickness of the rubber pads) are analysed in detail in both vertical compression (elastic analysis) and simple shear in large deformations. Uniaxial and shear response of the seismic devices obtained numerically are finally critically compared, with the aim of evaluating the best compound to be used in practice.

2 CURED RUBBER MECHANICAL PROPERTIES AS A FUNCTION OF HARDNESS

At present, the influence of pads thickness in the seismic isolation performance of rubber bearings is not completely understood in terms of types of elastomers, optimal recipe, ingredients of vulcanization to be used to increase both the mechanical performance and reduce costs. In this paper, three different thicknesses of rubber pads are considered and the vertical stiffness of the isolators so obtained is evaluated in conjunction with the shear behavior.

As a matter of fact, the utilization of thick pads provides a decrease of the vertical stiffness, which obviously depends on the elastic modulus of the rubber used.

In general, the so-called static modulus of a rubber compound is obtained in standard stress-strain tests in which the samples are extended at the rate of 20 in/min. The dynamic modulus is measured while the sample is oscillated about some given strain or stress, usually under some fixed superimposed load. Hardness is a modulus measured at very small deformations, commonly obtained by means of the use of indenter devices.

The static moduli at 300% extension, the dynamic moduli and the hardness data have been extensively studied by Studebaker & Beatty (1978). Usually modulus and hardness of a stock are increased through the use of fillers. As a consequence, both modulus and hardness depend on the so called filler “structure” (or more specifically on carbon black structure) and cross-linking density. Dealing with commercial compounds, which are rather random and heterogeneous, it is difficult to collect data regarding Young modulus and hardness and draw any generalization.

The standard test method to have an idea of rubber mechanical properties still remains ASTMD2240, which deals with the penetration of a specified indentor forced into the material under specified conditions. The test is called “durometer test”.

Durometer, like many other hardness tests, measures the depth of an indentation in the material created by a given force on a standardized presser foot. This depth is dependent on the hardness of the material, its viscoelastic properties, the shape of the presser foot, and the duration of the test. ASTM D2240 durometers allows for a measurement of the initial hardness, or the indentation hardness after a given period of time. The basic test requires applying the force in a consistent manner, without shock, and measuring the hardness (depth of the indentation). If a timed hardness is desired, force is applied for the required time and then read. The material under test should be a minimum of 6.4 mm (.25 inch) thick.

There are some empirical formulas that correlate indentation hardness to penetration, elastic modulus and viscoelastic behavior of the material.

For instance, the following external force-hardness empirical law holds for a so called type A durometer:

$$\text{Force}: N = 0.550 + 0.075 H_A \quad (1)$$

where H_A is the hardness read on a type A durometer.

Conversely, for a so called type B durometer the following formula may be used:

$$\text{Force}: N = 0.4445 H_D \quad (2)$$

where H_D is the hardness reading on a type D.

The difference between type A and type D durometers stands exclusively on the geometry of

the device.

Type A durometer is a hardened steel rod with diameter 1.1- 1.4 mm, with a truncated 35° cone of diameter 0.79 mm. Type D durometer is a hardened steel rod having a diameter of 1.1- 1.4 mm, with a 30° conical point and 0.1 mm radius tip.

Under small deformations rubbers are linearly elastic solids. Because of the high modulus of bulk compression, about 2000MN/m^2, compared to the shear modulus G, about 0,2-5MN/m^2 (Tobolsky and Mark, 1971), they may be regarded as relatively incompressible. The elastic behavior under small strains can thus be described by a single elastic constant G, being Poisson's ratio very near to ½ and Young's modulus E equal to $3G$ with very good approximation.

In order to have the possibility to evaluated the relation between hardness and Young's modulus, first of all we have taken into consideration a semi empirical relation between the shore hardness and Young's modulus for elastomers that has been derived by Gent (1958; 1978). This relation has the following form:

$$E = \frac{0.0981(56 + 7.62336S)}{0.137505(254 - 2.54S)} \quad (3)$$

where E is the Young's modulus in MPa and S is the shore hardness. This relation gives a value of E equal to infinite at S=100, but departs from experimental data for S lower than 40.

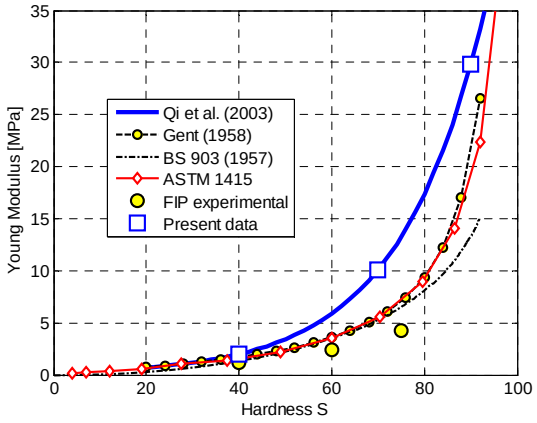

Figure 1: Empirical dependence of the rubber elastic modulus in terms of international hardness (formula (6). Circle, square and triangle denote elastic moduli used in the numerical simulations.

Another relation that fits experimental data slightly better is the following and is reported into British standards (BS 1950, BS 1957):

$$S = 100\ erf\left(3.186\times10^{-4}\sqrt{E}\right) \quad (4)$$

where *erf* is the error function and E is in units of Pa. A first order estimate of the relation between shore D hardness and the elastic modulus for a conical indenter with a 15 degree cone is:

$$S_D = 100 - \frac{20\left(-78.188 + \sqrt{6113.36 + 781.88E}\right)}{E} \quad (5)$$

where S_D is the shore D hardness and E is in MPa.

Another linear relation between the shore hardness and the natural logarithm of Young's modulus is applicable over a large range of shore A and shore D hardness (Qi et al., 2003). This relation has the form:

$$\ln(E) = 0.0235S - 0.6403 \quad (6)$$

Where S= S_A for S_A between 20 and 80 and S= S_D +50 for S_D between 30 and 85, being S_A the shore A hardness, S_D the shore D hardness and E the Young's modulus in MPa.

In our theoretical work, we have considered an ideal rubber item with different hardness and have calculated the corresponding Young's modulus. From that value, we have deduced the influence of the thickness of the compounding rubber materials for the optimal stiffness vertical resistance. However, hardness is a superficial determination and for this reason it is necessary to optimize also the density of cross-linking at same recipe. While this latter issue is extremely important, our work focuses on the possibility to increase the thickness of rubber pads to optimize the elastic properties of the items, such as initial compression modulus and shear behavior under large deformation.

The typical dependence of rubber Young modulus E with respect to hardness S, obtained by means of the empirical formulas discussed above is schematically represented in Figure 1.

As it is possible to notice and as expected, there is a quite large scatter of the results for rubbers with big hardness. However, formulas suggested by ASTM 1415 and BS 903 provide very similar results in a wide range, also for S near 80. Despite the fact that Qi et al., (2003) formula seems less conservative for hard rubbers, authors adopted such approach to evaluate Young modulus to use in the numerical simulations, being Qi et al., (2003) approach based on a convincing experimental and theoretical framework.

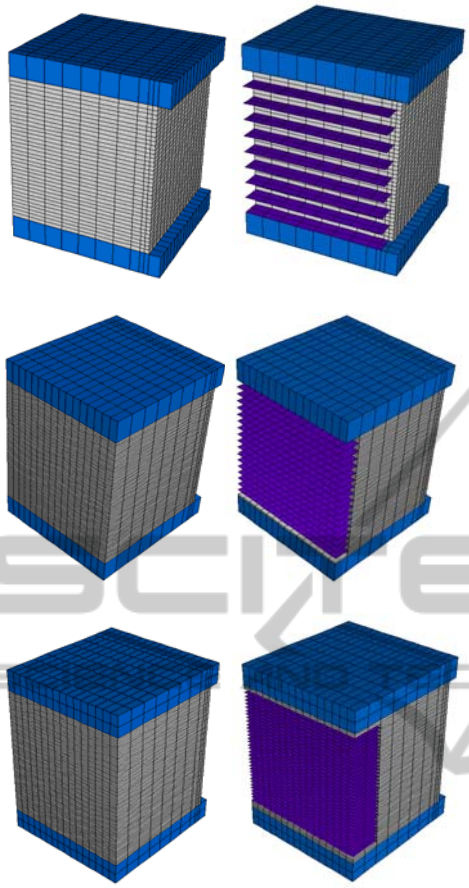

Figure 2: FE discretization of the seismic isolators studied.

3 NUMERICAL FINITE ELEMENT SIMULATIONS ON ELASTOMERIC ISOLATORS

One of the key parameters having a fundamental role in the determination of overall isolator compression elastic modulus E_c is the so called shape factor S_F (or primary shape factor), defined as the ratio between the loaded area and the lateral surface free to bulge. Since the shape factor refers to the single rubber layer, it represents a measure of the local slenderness of the elastomeric bearing. Experimental tests have shown that low shape factor bearings, characterized by values of S_F greater than 5 and less than 20 (in the present case S_F=7), provide an isolation effect in both the horizontal and vertical directions whereas high shape factor bearings, characterized by values of S_F greater than 20, only provide a good isolation in the horizontal direction. It is even obvious that low values of the shape factor define thick rubber layers and, hence, provide bearings characterized by high deformability. As a rule, in seismic isolation applications the need to have a device with a high vertical stiffness and low shear stiffness requires that S assumes values greater than 5 and less than 30.

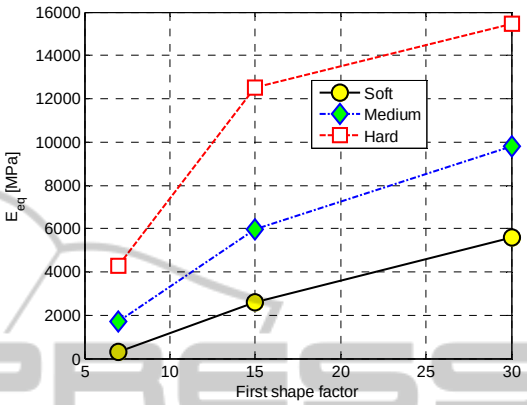

Figure 3: Isolator vertical elastic modulus varying shape factor and rubber hardness.

Three geometric cases corresponding to shape factors S_F equal to 7, 15 and 30 are hereafter considered. In these cases, the thicknesses of the single pad are approximately respectively equal to 5, 8.5 and 18 mm, assuming a width of the isolator equal to 500 mm (square isolators) and a total thickness equal to 250 mm. Assuming in the first case a thickness of steel laminas equal to 1 mm, in the second 2 mm and in the third 3 mm, the number of steel plates to be used on such devices is respectively equal to 38, 19 and 9.

Three refined discretizations are adopted in the numerical simulations discussed in this Section, as depicted in Figure 2. For rubber, eight-noded bricks elements are used, whereas for steel laminas four-noded plate and shell elements are adopted, to properly take into account both the in-plane and the out-of-plane effect induced by steel bending. Obviously, the isolator with shape factor S=30 requires several elements, due to the reduced thickness of the pads, namely 12224 bricks, 5328 plates and 14501 nodes.

Elastic analyses under small deformations are performed to characterize the vertical elastic modulus in compression, which is represented in

Figure 3, at different values of the shape factor and for the three blends represented in Figure 1 with squares.

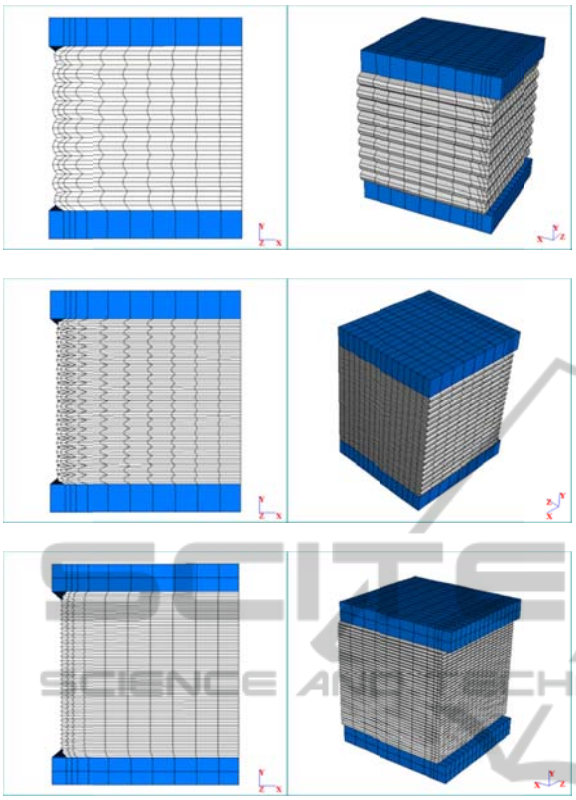

Figure 4: Deformed shapes for vertical compressions.

Obviously elastic modulus increases with shape factor and is maximum for the hard blend. Usually, elastic moduli of a seismic isolator should range between 1500 and 7500 MPa, meaning that for a shape factor equal to 15, a medium or a soft blend should be used. Conversely, for higher shape factor, soft blends could have the beneficial role to progressively decrease vertical stiffness, whereas for lower shape factors hard blends are preferable.

In Figure 4, deformed shapes of the three isolators under vertical compression are shown. The role played by the single rubber pad free to bulge is particularly evident.

To study the shear behaviour of the isolators under large deformations, a two constants Mooney-Rivlin model is utilized in what follows.

Defined the stretch as the ratio between the length in the deformed configuration divided by the length in the undeformed state, let $\lambda_1 = \lambda$ be the stretch in the direction of elongation and $\sigma_1 = \sigma$ the corresponding stress. The other two principal stresses are zero, since no lateral forces are applied $\sigma_2 = \sigma_3 = 0$. For constancy of volume, the incompressibility condition $\lambda_1\lambda_2\lambda_3 = 1$ gives:

$$\lambda_2 = \lambda_3 = \frac{1}{\sqrt{\lambda}} \tag{7}$$

The strain energy function for a two constats Mooney-Rivlin model is:

$$W = C_1(I_2 - 3) + C_2(I_1 - 3) \tag{8}$$

where $I_1 = \lambda_1^2 + \lambda_2^2 + \lambda_3^2$ and $I_2 = \lambda_1^{-2} + \lambda_2^{-2} + \lambda_3^{-2}$. Where C_1 and C_2 are material parameters to be determined for instance by a simple uniaxial tension test.

In uniaxial tension or compression equations (7) hold and therefore:

$$I_1 = \lambda^2 + \frac{2}{\lambda} \quad I_1 = 2\lambda + \frac{1}{\lambda^2} \tag{9}$$

The engineering stress S' (force per unit unstrained area of cross-section) in the case of an uniaxial tensile test may be evaluated from energy density as follows:

$$S' = 2\left(1 - \frac{1}{\lambda^3}\right)\left(\lambda\frac{\partial W}{\partial I_1} + \frac{\partial W}{\partial I_2}\right) \tag{10}$$

In simple shear deformation and differently to uniaxial compression, the direction of applied displacement does not coincide with the direction of principal stretches; rather it involves a rotation of axes. Due to applied shear strain γ, the deformation gradient tensor $\mathbf{F}$ and the left Cauchy-Green deformation tensor $\mathbf{B}$ are described as:

$$\mathbf{F} = \begin{bmatrix} 1 & \gamma & 0 \\ 0 & 1 & 0 \\ 0 & 0 & 1 \end{bmatrix} \quad \mathbf{B} = \begin{bmatrix} 1+\gamma^2 & \gamma & 0 \\ \gamma & 1 & 0 \\ 0 & 0 & 1 \end{bmatrix} \tag{11}$$

Consequently, the strain invariants are expressed as $I_1 = I_2 = 3 + \gamma^2$, $I_3 = 1$ and the expression for Cauchy stress becomes:

$$T_{12} = 2\gamma[\partial W / \partial I_1 + \partial W / \partial I_2] \tag{12}$$

In pure shear deformation principal stretches have the following form:

$$\begin{aligned} \lambda_1 &= \lambda \\ \lambda_2 &= \frac{1}{\lambda} \\ \lambda_3 &= 1 \end{aligned} \tag{13}$$

Consequently, the strain invariants are expressed as $I_1 = I_2 = \lambda^2 + 1/\lambda^2 + 1$ and the expression for Cauchy stress becomes:

$$\sigma_{11} - \sigma_{33} = 2C_1\left(\lambda^2 - 1\right) - 2C_2\left(\frac{1}{\lambda^2} - 1\right)$$

$$\sigma_{22} - \sigma_{33} = -2C_2\left(\lambda^2 - 1\right) + 2C_1\left(\frac{1}{\lambda^2} - 1\right) \qquad (14)$$

$$\sigma_{11} - \sigma_{22} = 2\left(C_1 + C_2\right)\left(\lambda^2 - \frac{1}{\lambda^2}\right)$$

The normal behaviour under large deformations of the single pad is shown in

Figure 5. Such a response under large deformations is fully determined once known the two Mooney-Rivlin constants C_1 and C_2. However, the initial Young Modulus gives only one information on such constants (G=2(C_1+C_2)). In what follows we therefore assume C_1=G/2 and C_2 =0, in absence of experimental data on constituent materials, which corresponds to a Neo-Hookean material.

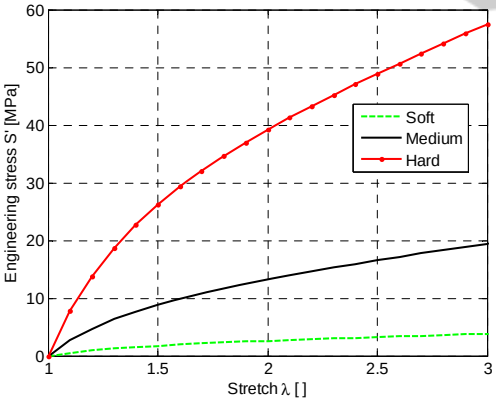

Figure 5: Stretch-stress behaviour of a single rubber pad (top) and pure shear behaviour under large deformations (bottom).

Having at disposal C_1 and C_2 constants, a standard large deformation software is utilized to plot the response of the whole isolator in shear, as sketched in Figure 6.

Figure 6 is particularly important for practical purposes, because the curves may be implemented at a structural level to study entire base-isolated buildings in the dynamic range.

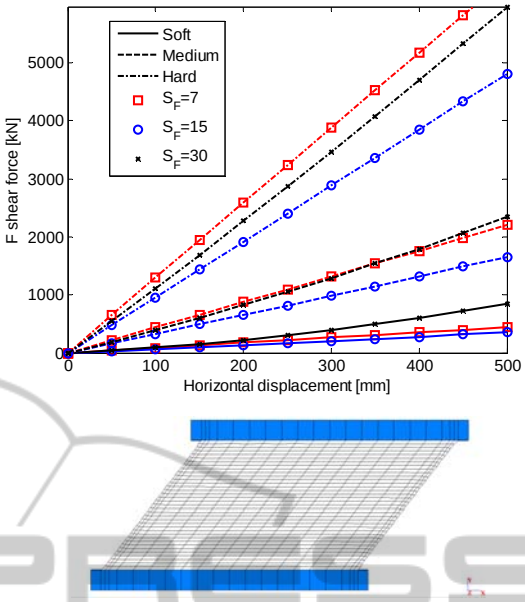

Figure 6: Force-displacement curves in shear under large deformations and corresponding deformed shape (S=7).

As it is possible to notice, the utilization of different hardness rubber pads in conjunction with slender or less slender isolators may considerably change the macroscopic response of the isolator and, hence, the effectiveness of the device inserted in a large case structure may be variable.

4 CONCLUSIONS

The important matter of the role played by the thickness of rubber pads within seismic isolators is not well covered in the literature. From our theoretical investigation, it is shown that a proper calculation is needed when the item involves a high thickness and a large volume of the elastomer compounds. Hardness is a very important parameter to define rubber initial Young's modulus, that is the main parameter to define the possibility that a predetermined thickness of the rubber pad is able to suitably support the vertical load. As it is known, the hardness determination, in general, is done on the surface of the items and this is function, at same recipe and rubber type, of the cross-link density. For this reason it will be required to deepen such preliminary results considering a particular rubber type, an experimental recipe and a mathematical approach to define the optimal vulcanization time/temperature and subsequently link these parameters with the hardness, to evaluate an optimal

cross-link density in any point of the items, especially for isolators with big dimensions.

Another important parameter that will be investigate is the hysteresis loss and thermo-mechanical behavior that, as known, can be correlated to the dynamic behavior based on cross-link structures. Finally, it will be considered the aging or the stability of the rubber items, that in general depends on the structure of the elastomer used. In our theoretical work it is shown that a proper calculation is needed when a product involves a large volume of the rubber items in the seismic isolators. It is suggested to consider the following steps for a choice of the optimal thickness of the pads as a function of predetermined hardness, which also allows to increase the volume of rubber and decrease the number of the steel plates:

1) Calculation of the Young's modulus from hardness.

2) Calculation of the maximum vertical stiffness supported.

3) Determination of the stretch-stress behaviour of the single rubber pad.

4) Determination of the shear behaviour of the whole isolator under large deformations.

5) Utilization of the stretch-stress and the shear behaviour in order to define the best solution for a single building.

6) Combination of the technical characteristics of the rubber pads and the steel laminas to minimize the cost, in order to introduce the seismic isolation technology in large buildings in high seismicity countries. The authors are convinced that this approach could be in the future the normal routine to design new buildings.

REFERENCES

Amin, A. F. M. S., Alam, M. S., Okui, Y., 2002. An improved hyperelasticity relation in modeling viscoelasicity response of natural and high damping rubbers in compression: experiments, parameter identification and numerical verification. *Mech. Mater*. 34: 74-95.

Amin, A. F. M. S., Wiraguna, I., Bhuiyan, A. R., Okui, Y., 2006. Hyperelasticity Model for Finite Element Analysis of Natural and High Damping Rubbers in Compression and shear. *Journal of Engineering Mechanics ASCE*, 132(1): 54-64.

British Standard 903, 1950, 1957. *Methods of testing vulcanized rubber*, Part 19 (1950) and Part A7 (1957).

Gent, A. N., 1958. On the relation between indentation hardness and Young's modulus. Institution of Rubber Industry – *Transactions*, 34: 46-57.

Gent, A. N., 1978. Rubber elasticity: basic concepts and behavior. In: *Science and Technology Rubber* (Ed.: F. R. Eirich), Academic Press, NY, San Francisco, London.

Gracia, L. A., Liarte, E., Pelegay, J. L., Calvo, B., 2010. Finite Element simulation of the hysteretic behavior on industrial rubber. Application to design rubber components. *Finite Elements in Analysis and Design* 46: 357-368.

Milani, G., Milani, F., 2012. Stretch-stress behavior of elastomeric isolators with different rubber materials. A numerical insight. J*ournal of Engineering Mechanics ASCE*, in press.

Moon, B. Y., Kanga, G. J., Kanga, B. S., Kim, G. S., Kelly, J. M., 2003. Mechanical properties of seismic isolation system with fiber-reinforced bearing of strip type. *International Applied Mechanics*, 39(10): 1231-1239.

Moon, B. Y., Kanga, G. J., Kanga, B. S., Kim, G. S., Kelly, J. M., 2002. Design and manufacturing of fiber reinforced elastomeric isolator for seismic isolation. *Journal of Materials Processing Technology*, 130-131: 145-150.

Qi, H. J., Joyce, K., Boyce, M.C., 2003. Durometer hardness and the stress-strain behavior of elastomeric materials. *Rubber Chemistry and Technology*, 72(2): 419-435.

Studebaker, M. L., Beatty, J. R., 1978. The rubber compound and its composition. In: *Science and Technology of Rubber* (Ed.: F.R. Eirich), Academic Press, NY, San Francisco, London.

Tobolsky, A. V., Mark, H. F., 1971. *Polymer Science and Materials*. Chap.13 (Ed.: Wiley) New York.

Tsai, H. S., Kelly, J. M., 2002. Stiffness Analysis of Fiber-Reinforced Rectangular Seismic Isolators. *Journal of Engineering Mechanics ASCE*, 128(4): 462-470.